Journal of Inorganic and Organometallic Polymers and Materials
https://doi.org/10.1007/s10904-024-03100-9

RESEARCH

Phytochemical Profiling of *Phragmites australis* Leaf Extract and Its Nano-Structural Antioxidant, Antimicrobial, and Anticancer Activities

Jeremiah O. Unuofin[1] · Adewale O. Oladipo[1] · Garland K. More[2] · Adeyemi O. Adeeyo[3] · Hassan T. Mustapha[4] · Titus A. M. Msagati[3] · Sogolo L. Lebelo[1]

Received: 12 March 2024 / Accepted: 4 April 2024

Abstract
Freshwater macrophytes have attracted interest as an alternative source of natural extracts and minerals for a variety of therapeutic uses. However, few studies have rigorously investigated the phytochemical components, properties, and potential biological benefits of *Phragmites australis* as an emergent macrophyte. This study investigates the phytochemical profile of aqueous *Phragmites australis* (PAE) leaves extract using chromatographic-mass spectrometry and free radical scavenging analysis. LC-QToF-MS/MS analysis in both positive and negative ionization revealed the existence of thirty and eleven bioactive compounds, respectively tentatively identified as alkaloids, flavonoids, indoles, glycosides, and quinolines from the extract. The polyphenolic content of the PAE was found to be 39.17 ± 0.65 mg GAE/g total phenol, while the flavonoids content was 19.85 ± 2.64 mg QE/g, and proanthocyanins content was 119.65 ± 1.70 CE/g. The PAE was utilized to synthesize silver nanoparticles (AgNPs) to evaluate its nano-structural formation efficiency, with the PAE displaying a greater ability to scavenge free radicals against ABTS, DPPH, and FRAP when compared with PA-AgNPs. Both PAE and PA-AgNPs were tested for their antimicrobial and anticancer activities and the results indicated that PA-AgNPs (MIC value range of 7.8–62.5 µg/mL) had excellent antimicrobial activity, compared to PAE. Moreover, the antiproliferative effect of PA-AgNPs on human cancer cells showed a higher cell-specific dose response and two-fold apoptotic induction with increased phosphorylation in the DNA ss-strand break post-treatment in MCF-7 than in A549 cells. These findings reveal the potential of the leaf extract of PA as a potent antioxidant source for many biological applications.

Keywords Silver nanoparticles · *Phragmites australis* · Antibacterial activity · Apoptosis · DNA damage

1 Introduction

Phragmites australis is a perennial grass found in temperate and tropical parts of the world. It is an aggressive, vigorous species with widespread growth in aquatic and semi-aquatic environments, especially in riverbeds and wet places. With little moisture, *P. australis* forms dense and dominant stands, growing as high as 4 m with long rhizomes, which makes them outcompete other local species [1]. In South Africa, it usually blossoms around December to June and has adapted to many ecosystems due to its resistance to low temperature, drought, and salinity, hence becomes difficult to control [2, 3]. The growth of *P. australis* is highly invasive, denying space and nutrients to fishes, plants, and wildlife as well as obstructing access to water for recreational activities like swimming and fishing. Additionally, invasive plants like *P. australis* raise the possibility of flooding and soil erosion, which can result in muddy water, poorer water

✉ Adewale O. Oladipo
oladiao@unisa.ac.za

[1] Department of Life and Consumer Sciences, College of Agriculture and Environmental Sciences, University of South Africa, Private Bag X06, Florida 1710, South Africa

[2] College of Agriculture and Environmental Sciences Laboratory, University of South Africa, Private Bag X06, Florida 1710, South Africa

[3] Institute for Nanotechnology and Water Sustainability (iNanoWS), College of Science, Engineering and Technology, University of South Africa, Private Bag X06, Florida 1710, South Africa

[4] Department of Chemical Sciences, Crescent University, Abeokuta, Ogun state, Nigeria

Published online: 10 May 2024

quality, and silted spawning areas [4]. It is usually spread by soil transfer, wind-brown seeds, animals, or large underground/aboveground branches. Even when the rhizomes are broken or destroyed, they can re-sprout in poor oxygen conditions and are of no grazing value [5]. Moreover, the dried plant material is often susceptible to fire with the potential to cause an environmental hazard from the emission of carbon monoxide and smoke, thus making it an environmental menace.

Regardless of the environmental problems posed by *P. australis*, humans have found it beneficial for numerous social and economic purposes. For centuries, people have utilized the stems of *P. australis* for fencing, roofing, insulation, and other purposes [6, 7]. Natives in Africa have utilized the plant for light baskets, weaving rods, mats, nets, prayer sticks, arrows, and fabrication works [8, 9]. Also, cellulose extracted from the plants has been used to produce cardboard and paper making [10, 11]. Today, *P. australis* has been used in phytoremediation wastewater treatment to remove heavy metals, micropollutants, nutrients, sediments, and emerging contaminants [12–15]. Besides, in Chinese herbal medicine, the dried *P. australis* rhizome has long been used to relieve fever and vomiting, induce diuresis, treatment of hepatitis, and suppress skin aging [3, 16, 17].

Recently, the utilization of *P. australis* has been driven by their potential source of bioactive agents for many biological applications. A review of the literature showed the fascinating biological activities of *Phragmites* species native to different countries. For instance, Chen et al. reported that alkaloids isolated from the roots of *P. australis* (Cav.) Trin. ex Steud. showed moderate cytotoxicity towards HeLa cells [18]. Sim et al. demonstrated that natural antioxidants present in water extracts of young leaves of *P. communis* may play several roles in suppressing melanogenesis and oxidative damage by downregulating melanogenesis-related gene expression [19]. Similarly, endophytes isolated from the roots of *P. australis* inhibited multi-drug resistant pathogens while aqueous extract from the rhizome showed antioxidant and hepatoprotective activities [17]. Apart from being a source of a wide range of natural products, its extracts and isolates have found tremendous application in the green synthesis of nanoparticles for the treatment of various diseases [20–22]. Interestingly, integrating nanoparticles into biomolecules to generate hybrid systems has become increasingly desirable in nanomedicine. The adsorption of bioactive compounds of plant origin onto the surface of nanoparticles confers fascinating properties such as large surface area, rapid electron transfer, enhanced surface binding, improved surface plasmonic properties, synergistic effects, etc [22–24]. Beyond these properties, the utilization of bioactive compounds derived from plant extracts presents an effective surface passivation strategy with distinctive reducing capabilities required for the preparation and functionalization of nanoparticles [24, 25]. This has been attributed to the highly ionizable functional groups (hydroxyl, carboxylic, phenolic, amine, etc.) present in the plant bioactive compounds [1]. Hence, the utilization of phytochemicals is beneficial for an alternative, facile, safe, cost-effective, and biocompatible nanoparticle synthesis.

To date, a few studies have been undertaken to utilize extracts from the *P. australis* plant for the synthesis of nanoparticles. Some research work utilized extracts from the rhizome and root of *P. australis* to synthesize gold nanoparticles [26], bimetallic gold-platinum [27], and copper oxide nanoparticles [28]. Besides, reports on the investigation of the chemical composition, properties, and biological and nano-structural activities of *P. australis* species in South Africa are limited. In this context, the advancements presented by nanotechnology in the management and treatment of human clinical pathogens and cancer could be explored by utilizing the extracts from *P. australis* leaves. The significance of this study entails the use of extract from this plant as an effective strategy for developing nanotherapeutic agents for combating not just antibiotic-resistant pathogens but also inflammatory diseases like cancer. Particularly, a major challenge in cancer treatment lies in the poor absorption of anticancer drugs after administration, thereby making sufficient accumulation at the diseased site difficult [29]. The bioavailability of natural compounds with potent antioxidant properties from plant extracts, aided by nano-based agents could improve cancer treatment outcomes. Therefore, in this study, we analyzed the metabolites present in the leaves of *P. australis* using liquid chromatography integrated into mass spectroscopy (LC-MS) and investigated the potential nano-silver antioxidant, antimicrobial activities as well as the anticancer mechanism. It is anticipated that using *P. australis* biomass for nanoparticle synthesis should provide an alternative to controlling and managing its environmental menace. Therefore, this study not only closes a significant gap in the scientific literature but also opens the door for novel treatment approaches to combat antibiotic-resistant bacteria and cancer.

2 Experimental

2.1 Materials and Chemicals

Phragmites australis leaves were collected from the Florida Lake area (latitude 26°10'16.2" S and longitude 27°53'39.6" E) in Gauteng province, South Africa. The leaves were identified at the Horticulture Centre, College of Agriculture and Environmental Sciences, University of South Africa. All the

chemicals used in this study were of analytical grade and were purchased from Merck, Johannesburg, South Africa.

2.2 Preparation of Leaves and Extract

The whole leaf powder was prepared as earlier reported [27]. In traditional medicine, a very common method for extracting bioactive compounds from herbs and leaves is to boil them in water. 10 g of leaf powder was added to 200 mL of MilliQ water and heated at 60 °C under magnetic stirring for 20 min. After cooling, the solution was filtered using Whatman filter paper, and the obtained extract was stored at 4 °C.

2.3 Preparation of Silver Nanoparticles

Silver nanoparticles (AgNPs) were prepared via a facile and eco-friendly approach using the extract of *Phragmites australis* (PAE). Briefly, 20 mL of extract was added to 100 mL 1 mM $AgNO_3$ solution in a flask and stirred at 60 °C for 1 h. The reaction was carried out in the dark to avoid unnecessary light interactions. After cooling, the solution was centrifuged at 4,400 rpm for 25 min, followed by washing with MilliQ water several times to remove unreacted extracts and precursor. The obtained pellets of AgNPs were dried overnight in an oven at 50 °C.

2.4 Characterizations

2.4.1 LC-QToF-MS/MS Analysis

Metabolites present in the aqueous extract of *P. australis* were investigated using LC-QToF-MS/MS in the positive and negative modes of ionization. 1 mg of dried PAE was dispersed in 1 mL of LC-MS grade water and sonicated for 10 min. The aqueous solution was filtered through a 0.22 mm polyvinylidene fluoride (PVDF) membrane filter and the obtained solution was analyzed for metabolites present using a high-resolution Impact II Quadrupole-time of flight mass spectrometer (QToF-MS) (Bruker, Germany). Data analysis was done using Compass Data Analysis software v4.3 (Bruker Daltonics, Germany) and the MetFrag web tool was used to compare the fragment patterns of ions obtained with those from KEGG and ChEBI databases [20].

2.4.2 UV-Visible Spectroscopic Analysis

The absorption spectra of PAE and synthesized PA-AgNPs aqueous suspension were monitored with a double-beam UV-visible spectrophotometer (Perkin Elmer Lambda 60) at a resolution of 1 nm and scanned at a range of 250–650 nm wavelength [30].

2.4.3 Fourier Transform Infrared Spectroscopy (FTIR)

The functional groups present in the PAE that were responsible for the stabilization and reduction of the synthesized PA-AgNPs were studied using FTIR analysis. PAE and PA-AgNPs dried at 50 °C overnight to remove any inherent water molecules present were scanned with a PerkinElmer Frontier FTIR fitted with an ATR detector in the range 4000–500 cm^{-1} [30].

2.4.4 Transmission Electron Microscopy (TEM), Selected Area Electron Diffraction (SAED), and Energy Dispersive X-ray Spectroscopy (EDS)

To investigate the structural properties of the PA-AgNPs, colloidal dispersion of the nanoparticles was made. After sonication for 10 min, a 5 µL diluted sample was placed onto a carbon-coated copper grid and allowed to dry. Thereafter, the sample was scanned using a transmission electron microscope, TEM (JEOL JEM 2100) running on a 200-kV voltage, and images were taken. A selected-area electron diffractogram was employed to assess the PA-AgNPs crystallinity. Additionally, the elemental composition of the PA-AgNPs was determined through an energy-dispersive X-ray analyzer (EDX) fitted to the TEM [31].

2.4.5 Dynamic Light Scattering and Zeta Potential Analysis

A homogenous suspension of the dried PA-AgNPs was obtained by ultrasonication for 10 min. The diluted suspension was analyzed for hydrodynamic diameter, polydispersity index (PDI), and surface charge using the Dynamic Light Scattering (DLS) approach (Malvern Zetasizer (Nano-ZS, Malvern, UK) [32].

2.5 Polyphenolic Content Quantification

Polyphenolic contents such as total phenol, flavonoids, and proanthocyanidins were quantified in the PAE and PA-AgNPs. These contents were evaluated according to the methods described [33, 34].

2.5.1 Antioxidant Activity

For this study we evaluated the radical scavenging capacities of PAE and PA-AgNPs using three antioxidant assays (2,2′-azino-bis (3-ethylbenzothiazoline)-6-sulfonic acid), 2,2-diphenyl-1-picrylhydrazyl), and ferric reducing antioxidant power). These antioxidant assays were performed according to methods adopted from previous studies [35, 36].

2.6 Antibacterial Screening

Antibacterial activity was tested against five bacterial strains *Staphylococcus aureus* (ATCC: 25,923), *Bacillus cereus* (ATCC: 10,876), *Escherichia coli* (ATCC: 25,922), *Enterobacter cloacae* (ATCC: 700,221), and *Salmonella Typhimurium* (ATCC: 39,183) purchased from Microbiologics® KWIK STIK™ (ANATECH, South Africa). All bacterial strains were grown and maintained in sterile nutrient agar and nutrient broth bought from Sigma-Aldrich® (Darmstadt, Germany) at 37 ºC in an incubator for 24 h.

2.6.1 Antimicrobial Activity

The serial dilution method was used for the determination of minimum inhibitory concentration (MIC) of the PAE and PA-AgNPs with ciprofloxacin and streptomycin as standard drugs (positive control) against five microbial species which are *Staphylococcus aureus*, *Bacillus cereus*, *Enterobacter cloacae*, *Escherichia coli* and *Salmonella typhimurium*. Stock solutions (1000 µg/mL) of PAE and PA-AgNPs were prepared in ultrapure water. Before the test, microorganisms were streaked on nutrient agar plates and incubated at 37 °C for 24 h. Pure microbe colonies were collected by a loop inoculated in sterile 10 mL sterile nutrient broth and incubated at 37 °C in a shaker for 24 h. A working stock of the culture was prepared by diluting the bacterial culture (1 µL:100 mL) *v/v* in broth. 100 µL of sterile distilled water was added to all the wells of a 96-well microplate. Followed by the addition of 100 µL of the samples, which were two-fold serially diluted, and 100 µL of bacteria was then added in all the wells including the positive control wells. The sample concentrations range of 250 to 2.0 µg/mL were obtained. Ciprofloxacin and streptomycin were tested at a concentration range of 25 to 0.2 µg/mL. After 24 h incubation, resazurin (10 µL of 0.2 mg/mL), an indicator of bacterial growth was added, and the resulting mixture was further incubated for 1 h. When resazurin is reduced to resorufin, the solution turns a bright pink (formation of formazan) which signifies viable bacteria. A dark blue color indicates bacterial inhibition. The MIC is defined as the lowest antibacterial concentration that maintains a blue color with resazurin. The MICs were determined as the concentration at which observable growth was inhibited. All experiments were performed in triplicates with two technical repeats [37].

2.7 Cell Cultures

Human breast carcinoma (MCF-7) and human lung carcinoma (A549) cell lines were obtained from CELLONEX, Johannesburg, South Africa. Cells were cultured in Dulbecco's Modified Eagle's medium (DMEM) supplemented with 10% fetal bovine serum (FBS), 1% Penicillin–streptomycin, and 1% Glutamine (Gln) (Merck, Johannesburg, South Africa) at 37 °C in a humidified incubator.

2.7.1 Cytotoxicity Assay

MCF-7 and A549 cells were seeded in 96-well plates (2×10^4 cells/well) at 50 µL/well. The viability of the cells treated with PAE and PA-AgNPs (0, 5, 10, 25, 50, 100, and 200 µg/mL) for 24 h was evaluated using CellTiter-Blue reagent (Promega, Madison, WI, USA). Fluorescence values from the experiments were recorded according to the manufacturer's guide using an ELISA microplate reader (ThermoFisher Scientific, Varioskan Flash, Vantaar, Finland), and the cell viability of the triplicate results were calculated.

2.7.2 Apoptosis Assay

Human cancer cell lines MCF-7 and A549 were treated with PAE and PA-AgNPs for 12 h at individual IC_{50} concentrations based on cytotoxicity assay results. PAE and AgNPs-induced apoptosis were determined using MUSE Annexin V and Dead Cell Assay Kit (EMD Millipore Corp., MA, USA) and analyzed with a GUAVA MUSE Cell Analyzer as described [38].

2.7.3 DNA Damage Assay

Multi-color DNA damage assay (analysis of DNA double-strand breaks) was evaluated upon treatment of MCF-7 and A549 with PAE and PA-AgNPs for 12 h at individual IC_{50} concentrations. The percentage of micronuclei production in treated cells was investigated using the GUAVA MUSE Cell Analyzer. The activation status of ATM and H2A.X was analyzed using the Multi-Color DNA damage kit (Luminex Corp., Austin, TX, USA) as described [39].

2.8 Statistical Analysis

Data were expressed as mean ± standard deviation (SD) of three independent experiments. Statistical analysis was done using MINITAB 17 and GraphPad Prism 8 with student t-test for comparison. The difference between the mean values of groups was considered significant at $*P < 0.05$.

3 Results and Discussions

3.1 Phytocompound Determination by LC-QToF-MS/MS Analysis in Positive Ionization

The investigation of the chemical compounds present in the aqueous *Phragmites australis* extract (PAE) was done using LC-QToF-MS/MS in both positive and negative ionization modes. Annotation was carried out based on the outcome of LC-QToF-MS/MS, the information from the online databases, and fragmentation in the previous literature. The LC-QToF-MS/MS profile revealed the presence of 30 major compounds from the positive mode which were summarized along with their retention time, tentative identification, chemical classification, molecular ion, and fragmentation data present in the *P*AE (Table 1). These compounds consist of phenols, saponins, glycosides, alkaloids, flavonoids, quinic acids and derivatives, medium-chain fatty acids, long-chain fatty acids, steroidal glycosides, resorcinols, phenylmethylamines, and fatty amides. The biological importance of some active compounds derived from the positive mode is tabulated in Table 2. Few compounds such

Table 1 LC-ToF-MS/MS positive ion mode analysis of aqueous leaf extract of *Phragmites australis*

Retention time (min)	Molecular Formula	Average mass	Tentative identification	Chemical classification	MS1 isotopic spectrum	MS/MS (m/z) fragment ions
5.620	$C_{11}H_{14}N_2O_2$	207.113	Phenylethylmalonamide	Phenylacetamides	208.107	44.052; 87.030; 126.047; 153.061; 207.108
6.590	$C_9H_{11}NO_2$	166.087	Gentiatibetine	Phenylalanine and derivatives	167.091	40.763; 61.365; 166.090; 166.478
6.641	$C_9H_{11}NO_2$	166.087	Benzocaine	Benzoic acid esters	167.090	73.442; 94.131; 124.731; 166.470
6.935	$C_{10}H_9NO$	160.076	Echinopsine	Hydroquinolones	161.073	58.066; 89.038; 125.010; 159.090
6.938	$C_{12}H_{16}N_2O$	205.134	N-Methylcytisine	Cytisine and derivatives	206.129 205.125 207.132	58.066; 105.068; 159.090; 205.129
7.131	$C_{15}H_{19}NO_6$	310.127	Sporovexin C	Cyanogenic glycosides	311.133	66.305; 117.071; 171.055; 213.93; 310.386
8.365	$C_{12}H_{16}N_2O$	205.132	Caulophylline	Quinolizidine alkaloid	206.136	59.052; 103.056; 151.034; 205.109
8.545	$C_{13}H_{16}N_2O$	217.133	Tetrahydroharmine	Harmala alkaloids	217.125	53.441; 114.778;161.061; 217.133
9.024	$C_{11}H_9NO_2$	188.07	Indoleacrylic acid	Indoles	189.075	49.486; 85.075; 122.523; 188.074
9.034	C_9H_7NO	146.059	Quinolin-8-ol	8-hydroxyquinolines	146.056	51.961; 91.049; 132.592; 145.080
9.043	$C_{11}H_{12}N_2O_2$	205.098	Vasicinol	Quinazolines	206.102	40.619; 101.175; 188.078; 205.101
9.421	$C_{13}H_{16}N_2O$	217.134	Girgensonine	Harmala alkaloids	217.126	44.052; 97.024; 150.957; 217.183
11.123	$C_{12}H_{12}N_2O_2$	217.098	Mansouramycin A	Isoquinoline	218.101	41.311; 61.687; 153.516; 217.128
12.116	$C_{10}H_8O_3$	177.054	4-Methylumbelliferone	7-hydroxycoumarins	177.048	58.062; 89.034; 128.074; 177.115
12.525	$C_{11}H_{14}O_5$	227.091	Genipin	Iridoids and derivatives	227.082	55.019; 103.050; 155.061; 227.160
15.512	$C_{26}H_{28}O_{14}$	565.159	Corymboside	Flavonoid 8-C-glycosides	565.159	66.233; 184.116; 397.189; 562.569
15.761	$C_{21}H_{20}O_{11}$	449.109	Luteolin 7-glucoside	Flavonoid 8-C-glycosides	450.112	43.231; 178.112; 294.028; 449.391
17.490	$C_{17}H_{18}O_4$	287.128	Sativan	4'-O-methylated isoflavonoids	287.125	52.744; 132.109; 194.069; 287.130
17.493	$C_{19}H_{22}O_5$	331.154	Fragransol B	2-arylbenzofuran flavonoids	332.156	48.345; 118.077; 228.101; 331.156
18.923	$C_{23}H24O_{11}$	477.141	Pectolinarigenin 7-glucoside	Flavonoid-7-O-glycosides	477.139	52.325; 114.125; 214.110; 338.049; 477.162
19.384	$C_{17}H_{14}O_7$	331.08	3,7-Dimethylquercetin	7-O-methylated flavonoids	331.080	69.067; 117.057; 226.124; 331.286
20.747	$C_{17}H_{24}N_2O$	273.196	beta-obscurine	Indoles and derivatives	273.198	49.953; 108.053; 164.067; 273.190
22.837	$C_{18}H_{19}NO_4$	314.138	Laurolitsine	Aporphine alkaloid	314.139	44.983; 115.525; 215.140; 314.153
23.955	$C_{24}H_{28}N_2O_6$	441.202	Diferuloylputrescine	Hydroxycinnamic acids and derivatives	442.206	40.406; 158.901; 265.156; 441.196
24.232	$C_{38}H_{62}N_2O_{13}$	755.432	Withanamide C	Phenolic glycosides	756.436	40.458; 121.455; 363.156; 578.229; 755.501
24.521	$C_{11}H_{16}O_2$	181.122	Olivetol	Resorcinols	181.124	46.564; 76.902; 102.95624:13 120.565;181.131
24.544	$C_{23}H_{41}N$	332.331	Piptamine	Phenylmethylamines	334.337	40.173; 130.082; 230.135; 332.335
24.666	$C_{18}H_{35}NO$	282.278	Oleamide	Fatty amides	283.282	40.200; 108.087;198.131; 282.324
24.675	$C_{13}H_{24}N_2O$	225.196	Cuscohygrine	Alkaloids and derivatives	225.196	40.969; 91.054; 105.714; 150.116; 225.198

Table 2 Pharmacological activities of phytocompounds from positive ion mode analysis of aqueous leaf extract of *Phragmites australis*

Ingredients	Pharmacological activities	References
Phenylethylmalonamide	Possess anticonvulsant effect	[40]
Gentiatibetine	Exhibits anticonvulsant and brain-protective effects	[41]
Benzocaine	Possesses antibacterial and anticancer potential	[42]
Echinopsine	Herbicidal, insecticidal, bactericidal, anti-tumor, antifungal, and antifeedant activities	[43, 44]
N-methylcytosine (NMC)	Anti-inflammatory effects of N-methylcytosine (NMC) in a dextran sulfate sodium (DSS)-induced colitis model	[45]
Sporovexin C	Antifungal and antibacterial effects	[46]
Caulophylline	Exerts hypoglycaemic, analgesic, and anti-inflammatory activities	[45]
Tetrahydroharmine	Reported to have anxiolytic or anti-depressive and anti-inflammatory effects	[47, 48]
Indoleacrylic acid	Promotes anti-inflammatory responses	[49]
Quinolin-8-ol	Antimicrobial and antimalarial activities	[50]
Vasicinol	Possesses angiotensin-converting enzyme (ACE) inhibitory potential thus it exhibits great potential to alleviate hypertension	[51]
Girgensonine	Possess acetylcholinesterase inhibition and larvicidal activity	[52]
Mansouramycin A	Exhibit antibacterial activity.	[53]
4-Methylumbelliferone	Possess an antitumor effect against canine mammary tumor cells and also ameliorates hypertriglyceridemia and hyperglycemia via the modulation of hepatic lipid metabolism and the antioxidant defense system of high-fat diet-induced hypertriglyceridemia and hyperglycemia in mice.	[54, 55]
Genipin	Possesses numerous biological activities such as anti-inflammatory, anti-tumor, anti-coagulant, anti-hypertensive, and hypoglycemic activities.	[56–60]
Corymboside	Exhibit anti-inflammatory and antioxidative activities	[61]
Luteolin-7-O-glucoside	Possesses potential antibacterial, antifungal, antioxidant, and anti-inflammation effects	[62–64]
Sativan	Possesses antituberculosis activity and exerts anti-cancer effects on breast cancer cells	[65, 66]
Fragransol B	Possesses anti-inflammatory potential.	[67]
Pectolinarigenin 7-glucoside	Exert antioxidant and anti-cholinesterase activity	[68]
3,7-Dimethylquercetin	Exert anti-inflammatory effect in lipopolysaccharide-activated RAW 264.7 cells	[69]
Beta-obscurine	Exert anticancer activity against the human breast cancer cell line (MDA-MB-231).	[70]
Laurolitsine	Exert antihyperglycemic and antihyperlipidemic in Sprague-Dawley rats	[71]
Diferuloylputrescine	Possess antileukemic activity in human leukemia U937 cells	[72]
Withanamide C	Neutralize the toxicity of β-amyloid protein (BAP) and protect the cells from cell death	[73]
Olivetol	Possesses antioxidant and anticholinergic properties	[74]
Piptamine	Displayed antimicrobial activity against a series of Gram-positive bacteria, yeasts, and fungi.	[75]
Oleamide	Suppresses inflammatory responses in BV2 murine microglial cells and LPS-induced RAW264.7 murine macrophages	[76, 77]
Cuscohygrine	Hepato-renal protective properties against fibrosis	[78]

Table 3 LC-ToF-MS/MS negative ion mode analysis of aqueous leaf extract of *Phragmites australis*

Retention time (min)	Molecular Formula	Average mass	Tentative identification	Chemical classification	MS1 isotopic spectrum	MS/MS (m/z) fragment ions
9.305	$C_{16}H_{18}O_9$	353.0896	Scopoletin	Quinic acids and derivatives	354.0930	41.647; 156.695; 253.694; 309.346; 353.098
12.127	$C_{17}H_{20}O_9$	367.1020	4-O-feruloyl-D-quinic acid	Quinic acids and derivatives	368.1062	178.730; 224.661; 280.695; 364.778
12.544	$C_{17}H_{24}O_{10}$	387.1301	Geniposide	Iridoid O-glycosides	388.1320	147.061; 222.158; 302.639; 387.138
15.072	$C_{17}H_{20}O_9$	367.1049	3-O-Feruloylquinic acid	Quinic acids and derivatives	368.1174	77.471; 163.038; 231.371; 293.108; 367.142
15.519	$C_{26}H_{28}O_{14}$	563.1399	Corymboside	Flavonoid 8-C-glycosides	564.1572	42.619; 151.785; 296.971; 396.161; 563.150
15.766	$C_{21}H_{20}O_{11}$	447.0936	Luteolin 7-glucoside	Flavonoid-7-O-glycosides	448.0969	101.992; 213.381; 319.089; 447.097
17.498	$C_{27}H_{36}O_{13}$	567.20978	Lucidumoside D	Steroidal glycosides	568.2249	115.099; 369.685; 489.230; 567.163
18.932	$C_{23}H_{24}O_{11}$	475.12219	Pectolinarigenin 7-glucoside	Flavonoid C-glycosides	476.1255	41.106; 138.237; 228.883; 371.240; 475.125
19.478	$C_9H_{16}O_4$	187.09627	Eucommiol	Medium-chain fatty acids	188.1011	120.430; 150.830; 181.491; 187.092; 187.101
24.373	$C_{18}H_{34}O_5$	329.2321	Tianshic acid	Long-chain fatty acids	330.2357	44.801; 160.393; 265.108; 329.256

Table 4 Pharmacological activities of phytocompounds from negative ion mode analysis of aqueous leaf extract of *Phragmites australis*

Ingredients	Pharmacological activities	References
Scopoletin	In in vitro studies, pharmacological activities include anti-bacterial, anti-fungal, anti-tubercular, and anti-hypertensive properties	[79–81]
	In in vivo studies, pharmacological activity includes anti-inflammatory, neurological, and anti-diabetic properties	[82–84]
4-O-feruloyl-D-quinic acid	Possess antioxidant and anti-inflammatory properties in vitro	[85]
Geniposide	Possesses antitumor, wound healing, neuroprotective, hepatoprotective, and cholagogic effects	[86–89]
Lucidumoside D	Suppresses Hepatitis B virus (HBV)	[90]
Corymboside	Exhibit antitumoral and antitrypanosomal activities	[91]
Luteolin 7-Glucoside	Possesses antioxidant, anti-inflammatory, and anti-cancer activity	[92]
Pectolinarigenin 7-glucoside	Possess antioxidant and anticholinesterase activities	[68]
Eucommiol	promote hypnotic and sedative effects in mice	[93]

as Laurolitsine and Fragransol B are rarely detected in plant extracts and have diverse applications.

3.2 Phytocompound Determination by LC-QToF-MS/MS Analysis in Negative Ionization

The LC-QToF-MS/MS profile revealed the presence of 11 major compounds from the negative mode which were summarized along with their retention time, molecular formula, average mass, tentative identification, chemical classification, molecular ion, and fragmentation data present in the *P*AE (Table 3). The biological importance of some active compounds derived from the positive mode is tabulated in Table 4.

3.3 Characterization of PA-AgNPs

3.3.1 UV-Vis Spectroscopy

The synthesis of nanoparticles usually requires an electron-donor/accelerator source that can reduce metal ions to individual nanoparticles. Consequently, the PAE was used to evaluate the feasibility and effectiveness of the formation of nanoparticles. With numerous bioactive compounds capable of reducing metal ions as highlighted from the LC-MS analysis, the PAE could serve as a green, simple, and cost-effective stabilizing and reducing agent for the reduction of Ag ions, thus the formation of silver nanoparticles (PA-AgNPs). The primary indicator of the formation of AgNPs was the color shift from pale yellow to dark brown after 60 min reaction time (Fig S1). As shown in Fig. 1A, the absorption spectra of PAE and formed PA-AgNPs were analyzed using a UV-vis spectrometer. The PA-AgNPs spectrum showed the characteristic peak of Ag at 416 nm, corresponding to the surface plasmon resonance of AgNPs [94]. The additional peaks at 295, 324, 538, and 615 nm could be attributed to the strong adsorption of bioactive compounds from PAE to the nanoparticles. Similar observation revealed that the reduction, capping, and stability of AgNPs were facilitated by *Lagerstroemia speciosa* flower bud extract containing a variety of phytochemicals [31].

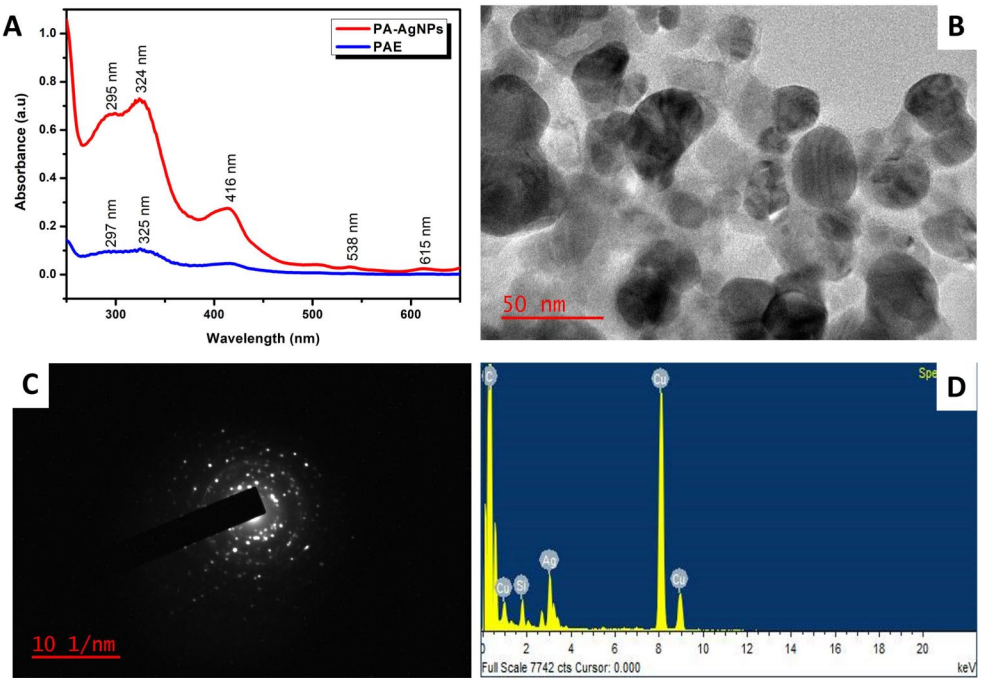

Fig. 1 (**A**) Absorption spectra (**B**) TEM image (inset: HRTEM), (**C**) SAED, and (**D**) EDX of PA-AgNPs

3.3.2 Morphological and Elemental Analysis

The shape and size of the PA-AgNPs were analyzed using transmission electron microscopy (TEM) and selected area diffraction (SAED). From Fig. 1B, the micrograph of the PA-AgNPs were mostly spherical (HRTEM inset) with a low occurrence of irregular shapes. An average particle diameter as measured from TEM was 38.4 ± 1.7 nm (less than 100 nm), known to be readily taken up by cells and can penetrate the nuclear membrane [35]. The occurrence of different shapes and sizes of nanoparticles could be due to the presence of various phytochemicals in the PAE [95]. Besides, the distinct appearance of the particles demonstrates the ability of the PAE to efficiently stabilize and prevent nanoparticle aggregation. The PA-AgNPs' selected area electron diffraction (SAED) pattern displayed many diffraction rings with bright dots encircling a single nanoparticle (Fig. 1C) which could be assigned to the face-cubic centered (fcc) crystalline nature of the formed nanoparticles. The energy-dispersive X-ray (EDX) spectroscopy was used to assess the elemental composition of the PA-AgNPs. As seen in Fig. 1D, the EDX spectrum indicated an Ag peak along with carbon and copper peaks from the carbon-coated copper grid. Therefore, the macromolecular phytochemicals present in the PAE enabled the formation of AgNPs with properties consistent with previous studies [96, 97].

3.3.3 Fourier-Transform Infrared Spectroscopy (FTIR)

FTIR spectroscopic technique was used to investigate the bioactive molecules from the PAE that might be involved

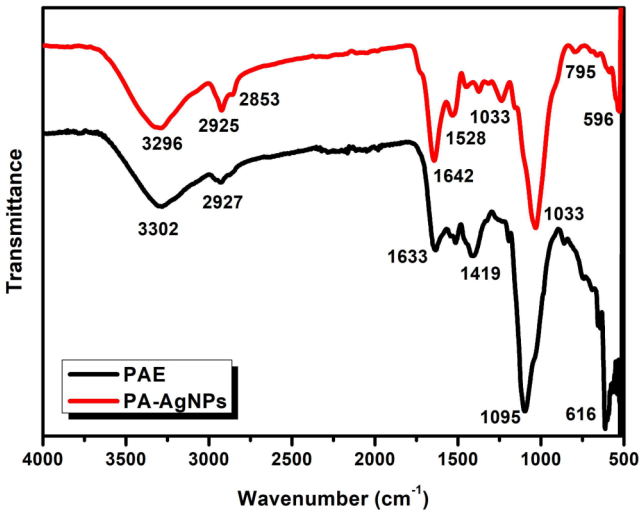

Fig. 2 FTIR spectra of aqueous PAE and synthesized PA-AgNPs

in the reduction and formation of AgNPs. From the analysis (Fig. 2), different vibrational peaks at 3302, 2927, 1633, 1419, and 1095 $cm-^{1}$ assigned to alcohols/phenols (–OH), C–H, C=C or C=N, C=O stretching, and C–O stretching, respectively were present in the PAE. These vibrational peaks were mostly detected in the spectrum of PA-AgNPs. For instance, a slight shift from 3302 to 3296 cm^{-1}, more pronounced asymmetric alkanes at 2925, 2853 cm^{-1}, tertiary amides at 1642, 1528, and 1033 cm^{-1} with new peaks at 1253, 795, and 596 cm^{-1} were all observed. The functional groups present in PAE showed similarity with those found in the root extract of *P. australis* [26]. These findings demonstrated that the phytochemicals present in the PAE

have a substantial capacity to interact with metal ions which mediated the stabilization and reduction of the PA-AgNPs.

3.3.4 Nanoparticle Stability

The stability of the colloidal PA-AgNPs was monitored using the Dynamic Light scattering technique. In this case, the PA-AgNPs were dispersed in deionized water and the hydrodynamic size, polydispersity index (PDI), and zeta potential were assessed for 5 days. As observed in Table S1, the PA-AgNPs indicated an average value of -28.2 ± 2.75 mV at the initial time and no significant change in all the parameters measured was noticed. The stability of nanoparticles in water has been linked to the surface adsorption of functional groups (–OH and –COOH) present in plant extracts which protects the nanoparticles from aggregating in solution. Besides, the high negative value and low PDI observed may suggest the long-term stability of the nanoparticles, thus making them beneficial for biological applications.

3.4 Analysis of Metabolites

3.4.1 Quantification of Polyphenolic Content

The highest total phenolic content was observed in PAE (39.17 ± 0.65 mg GAE/g) as compared to its synthesized PA-AgNPs (19.69 ± 0.28 mg GAE/g) as shown in Table 5. The total flavonoid content was slightly higher in PA-AgNPs (20.06 ± 0.51 mg QE/g) compared to those of PAE (19.85 ± 2.64 mg QE/g). In addition, the PA-AgNPs (313.15 ± 8.41 mg CE/g) had higher proanthocyanidin content when compared with the PAE (119.65 ± 1.70 mg CE/g) in Table 5. The availability of secondary metabolites such as polyphenolic compounds in plants is crucial for the reduction of metal ions into their corresponding nanosized metals [35, 98]. This confirms that not all the metabolites are used up for the reduction in the Ag salt, but also act as the capping agent [99]. Hence, the reason a higher total phenol content was observed in PAE when compared to the PA-AgNPs.

3.4.2 Antioxidant Potential

The free radical scavenging abilities of PAE and PA-AgNPs are shown in Table 6. One of the paths explored in measuring antioxidant capacity is the electron transfer mechanism [100]. This mechanism governs ABTS, DPPH, and FRAP radical scavenging capacities. Our study revealed that PAE had better free radical scavenging potential when compared to the PA-AgNPs against ABTS, DPPH, and FRAP radicals as presented in Table 6. These findings are in line with Demirbas et al. studies [101] which showed a reduced antioxidant capacity in AgNPs when compared with red cabbage extract (Brassica oleracea var. capitate f. rubra). In addition, lower antioxidant capacity was reported for green synthesis of AgNPs using *Aesculum hippocastanum* leaf extract when compared with plant extract using DPPH, total reducing power, and superoxide anion radical scavenging assay [102]. These results are of divergent views, as some authors observed a higher antioxidant capacity of AgNPs [103, 104]. Based on these two divergent types of results, it could be postulated that both scenarios are possible.

Table 5 Polyphenolic content estimated for PAE and PA-Ag NPs

Samples	Total Phenol Content (mg GAE/g)	Total Flavonoid Content (mg QE/g)	Proanthocyanidin (mg CE/g)
PAE	39.17 ± 0.65^{a}	19.85 ± 2.64^{a}	119.65 ± 1.70^{a}
PA-AgNPs	19.69 ± 0.28^{b}	20.06 ± 0.51^{b}	313.15 ± 8.41^{b}

Values are expressed as the mean of triplicate ± standard deviation. Different alphabets (a – b) within a column of a given parameter are significantly different at $P < 0.05$

Table 6 Comparative analysis of the antioxidant activity of PAE and PA-AgNPs

Samples	ABTS (µmol TE/g)	DPPH (µmol TE/g)	FRAP (µmol TE/g)
PAE	321.59 ± 7.24^{a}	147.83 ± 0.36^{a}	217.15 ± 4.55^{a}
PA-AgNPs	58.55 ± 2.94^{b}	8.84 ± 0.889^{b}	160.15 ± 1.70^{b}

Values are expressed as the mean of triplicate ± standard deviation. Different alphabets (a – b) within a column of a given parameter are significantly different at $P < 0.05$

3.5 Antibacterial Activity of PA-AgNPs

When evaluating the antibacterial efficacy of compounds using the resazurin assay, the noticeable color changes in resazurin were noted as the minimum inhibitory concentration (MIC). Resazurin is converted to resorufin by mitochondrial oxidoreductases; a pink color change indicates bacterial survival, whereas a dark blue color change indicates bacterial inhibition. By maintaining the blue color, the MIC was ascertained (Fig. 3). The study revealed that both the PAE and PA-AgNPs showed good antimicrobial activity against various microbial strains used. In general, the PA-AgNPs showed better activity by inhibiting all gram-positive (*S. aureus* and *B. cereus*) and gram-negative (*E. cloacae, E. coli, and S. typhimurium*) bacteria than PAE at MIC ≤ 62.5 µg/mL. Moreover, PAE exhibited the best results against *B. cereus* and *E. coli* with MIC = 62.5 µg/mL (Table 7). However, this study revealed that gram-negative bacteria were less susceptible to both samples compared to gram-positive. The conventional FDA-approved antibacterial drugs used in this study as positive control; ciprofloxacin and streptomycin showed excellent inhibitory results at MIC ≤ 1.95 µg/mL.

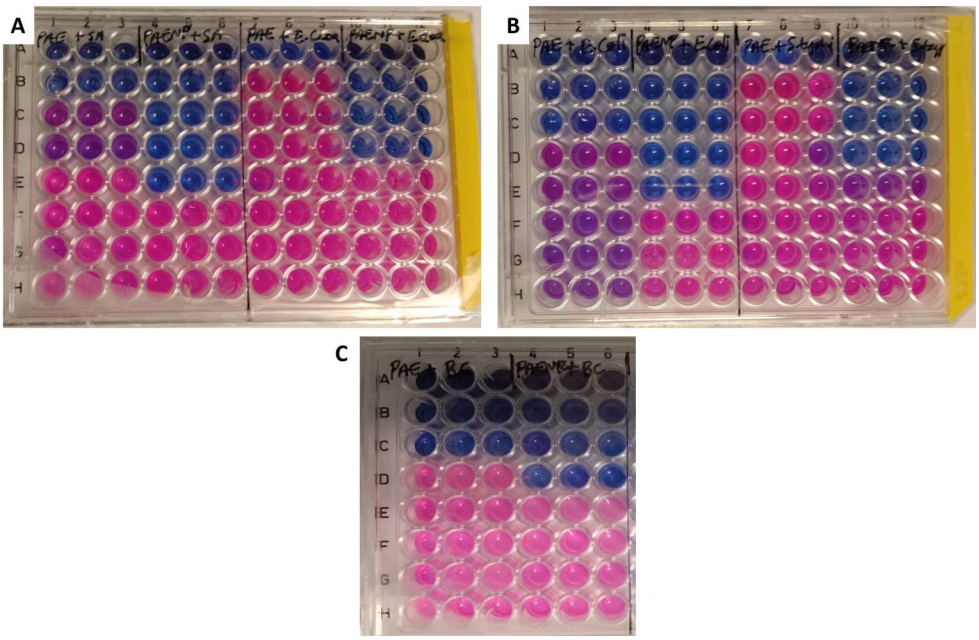

Fig. 3 The visual observation of antibacterial plates after 24 h incubation with PAE and PA-AgNPs. (**A**) *Staphylococcus aureus* and *Enterobacter cloacae*, (**B**) *Escherichia coli* and *Salmonella typhimurium*, and (**C**) *Bacillus cereus*. The pink and purple colors indicate microbial growth and inhibition, respectively

Table 7 Minimum inhibitory concentration (MIC) values representing the antimicrobial screening of the PAE and PA-AgNPs

Samples	MIC (µg/mL)				
	B. cereus	S. aureus	E. coli	E. cloacae	S. typhimurium
PAE	**62.5**	125.0	**62.5**	250.0	250.0
PA-AgNPs	**15.6**	**7.8**	**31.2**	**31.2**	**62.5**
Ciprofloxacin	0.8	0.8	2.0	6.0	0.4
Streptomycin	4.0	2.0	0.4	0.8	2.0

Bolded values are significant as noteworthy (MIC ≤ 62.5 µg/mL) antimicrobial activity

3.6 Anti-Proliferative Properties of PA-AgNPs on Cancer Cells

In this study, the toxicity effect of PAE and PA-AgNPs was evaluated against human breast (MCF-7) and lung (A549) cancer cell lines using a fluorometric assay. The results obtained showed that PAE did not show any noticeable reduction in the viability of both cells even at the highest concentration (Fig. 4). However, exposure of PA-AgNPs to MCF-7 cells showed a dose-dependent decrease in viability as concentration increases (Fig. 4A). The initial and highest concentration of PA-AgNPs reduced the viability by 35.6% and 93.4%, respectively. However, in A549 cells, there was no significant change in the viability of cells after exposure (Fig. 4B) as only PA-AgNPs at the highest concentration (200 µg/mL) reduced the viability by 37.5%. These results indicated that the PA-AgNPs are capable of penetrating the membrane of cells and interacting with intracellular components, thus significantly inhibiting the growth of MCF-7 cells even at low dosages. A half-maximal inhibitory concentration (IC_{50}) value for PAE and PA-AgNPs (74.68 and 11.47 µg/mL) and (> 100 and ~ 121.2 µg/mL) were calculated for MCF-7 and A549 cells, respectively (Table S2). The calculated IC_{50} value indicates that the PA-AgNPs are more efficient in causing significant cell death at a low dosage

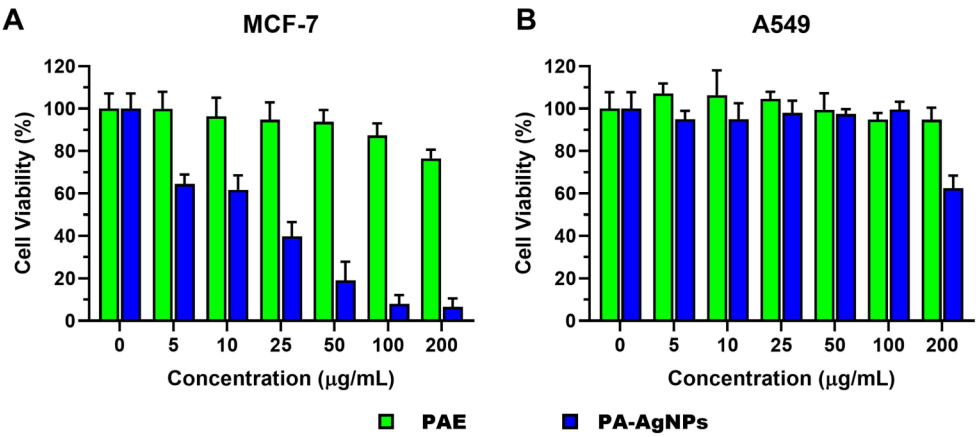

Fig. 4 Cell viability of (A) MCF-7 and (B) A549 carcinoma cells treated with PAE and PA-AgNPs

in MCF-7 than in A549 cells. The limited killing efficiency suggests that the PA-AgNPs may not possess anticancer/anti-proliferative properties in A549 cells. These findings from the cytotoxicity assay agreed with previous studies, which showed the cell-specific response of nanoparticles toward different cells at similar IC_{50} values [35]. Based on these results, we decided to look into whether apoptosis was the cause of the loss of viability post-exposure in both cancer cell types.

3.7 Apoptotic Induction Profile of PA-AgNPs on cancer Cells

Phosphatidylserine (PS), an apoptosis-induction biomarker, can be translocated to the outer leaflet of the membrane upon rupture of the plasma membrane, making it possible to determine the various stages of cell health. Based on this, the mechanism of cell death resulting from the inhibition of growth after exposure to PA and PA-AgNPs was investigated using flow cytometry. After labeling with Annexin V and Dead Cell reagent, MCF-7, and A549 cells treated with PAE (IC_{50} = 74.68 and 100 µg/mL) and PA-AgNPs (IC_{50} = 11.47 and 121.2 µg/mL), respectively, for 12 h, were examined for their apoptotic response. In Fig. 5, the apoptotic percentage increased to 26.9% for MCF-7 cells treated with PA-AgNPs compared to 9.2% in PAE. However, there was a reduction in apoptotic induction noticed in A549 cells treated with PA-AgNPs (12.9%) and PAE (9.0%). The results demonstrated that PA-AgNPs induced a two-fold apoptosis in MCF-7 than in A549 cells even at higher IC_{50} dosage. While PAE and PA-AgNPs both caused apoptosis, PA-AgNPs were more effective on MCF-7 cells ($^*P < 0.05$) than on A549 cells (Fig S2). It is commonly known that non-small cell lung cells, such as A549., are resistant to drugs and nanoparticles [105]. This is because the overexpression of lung-resistant proteins with cytoprotective properties has been primarily linked to their resistance to drug or nanoparticle absorption and transport [106, 107]. Moreover, the release of cytotoxic Ag ions, the mechanism of cell uptake, and the physicochemical properties of PA-AgNPs may have played a role in the selective response and enhanced apoptosis observed in MCF-7 cells [108].

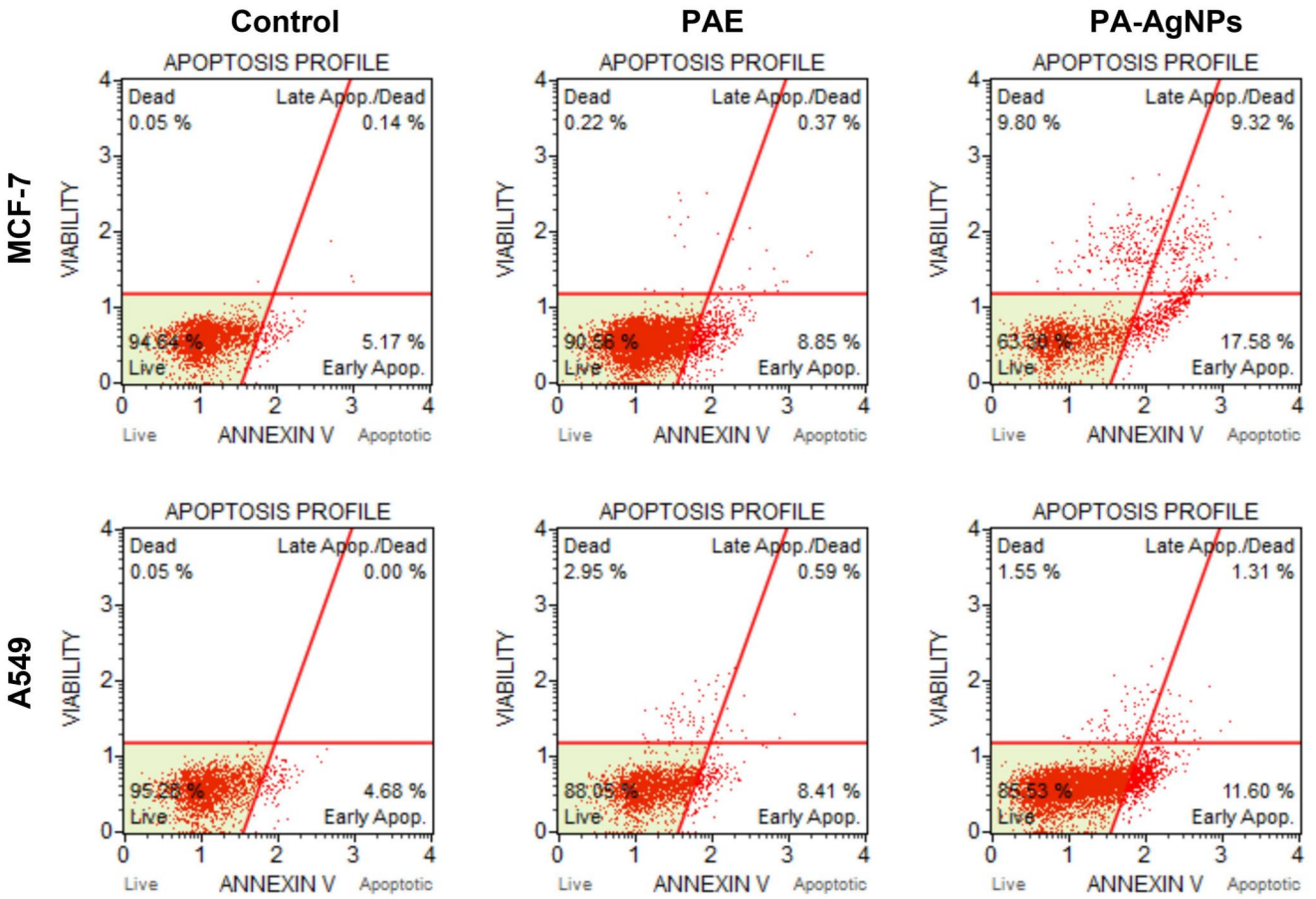

Fig. 5 Flow cytometry analysis of PAE and PA-AgNPs treatment on MCF-7 and A549 cells at 12 h

3.8 PA-AgNPs Induce DNA Damage on Cancer Cells

Phytochemicals including flavonoids, terpenes, isoflavones, and carotenoids with antioxidant properties have been implicated in the regulation and metabolism of various diseases including cancer. These phytochemicals could induce DNA damage via the activation of apoptosis due to their antioxidant properties [109]. In this study, it was discovered that treatment with PA-AgNPs induced DNA damage in the nucleus of cancer cells (Fig. 6). An increased phosphorylation of ATM and H2A.X levels in MCF-7 cells was observed compared to the control. The DNA double-strand (dual activation of ATM and H2A.X) and single-strand breaks (pATM) increased to (11.62 ± 1.02% an 66.16 ± 2.11%) i percentage compared to PAE (15.02 ± 2.72% an 13.50 ± 1.43%) ad control (2.36 ± 1.12% an 0.46 ± 1.07%) rspectively. However, moderate DNA damage was seen in A549 cells treated with both PAE and PA-AgNPs. The total DNA damage recorded for PAE and PA-AgNPs treatment was 10.14 ± 1.32% an 12.22 ± 1.09% copared to 7.11 ± 0.41% fo the control. It can be suggested that PA-AgNPs treatment promoted DNA damage in a cell-responsive manner as shown by higher ATM activation and H2A.X phosphorylation levels observed in MCF-7 cells, unlike A549 cells. Several studies have highlighted that extract-synthesized nanoparticles could induce DNA damage in the intracellular environment, which could interrupt genetic code transmission [110, 111]. The induction of apoptosis resulting from the damage to the nuclear component could play a role in regulating the antineoplastic effects of extract-mediated nanoparticles. Hence, it can be concluded that PA-AgNPs promote apoptosis by modulating DNA damage in cancer cells. The results of all experiments carried out provided sufficient evidence that PA-AgNPs effectively inhibited the proliferation of MCF-7 and A549 cells. From the current study, one of the contributing factors in the apoptotic induction of PA-AgNPs is the ROS-induced antioxidant properties. Therefore, it is possible that the synergy between the antioxidant properties of PAE and the physicochemical characteristics of PA-AgNPs enhanced its anticancer potential against cancer cells.

4 Conclusion

In this study, the limited popularity of *Phragmites australis* as a source of natural bioactive compounds motivated our investigation of their potential applications. The phytochemical screening identified thirty-one phytocompounds of

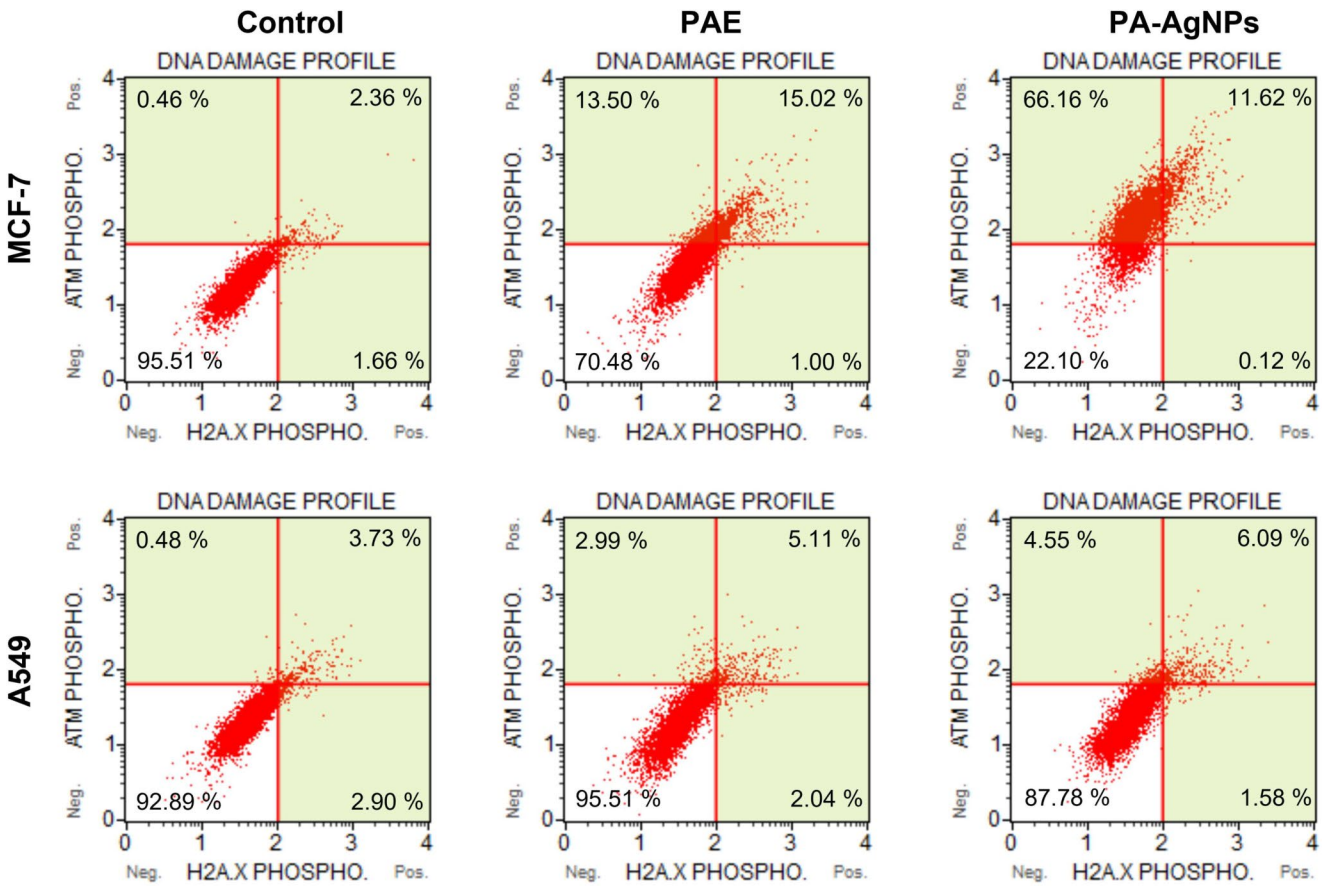

Fig. 6 DNA damage induced by the treatment of MCF-7 and A549 cells with PAE and PA-AgNPs for 24 h

immense pharmacological benefits in both positive and negative modes of ionization. Interestingly, the PAE was found to exhibit higher antioxidant properties due to its abundant bioactive compounds. Both the PAE and PA-AgNPs displayed good antimicrobial activities with the PA-AgNPs showing better antimicrobial activity than PAE. Besides, this study revealed that gram-positive bacteria were more susceptible to both samples. From the cell-based assays, a lower IC_{50} dose of PA-AgNPs was considerably effective against MCF-7 cells compared to A549 cells, demonstrating its anticancer and cell-specific response. Additionally, the flow cytometry method was used to assess apoptotic/necrotic induction against cancerous cells. The Annexin V & Dead and DNA damage assays were utilized to confirm that PA-AgNPs upregulated apoptosis and subsequent DNA damage of cancer cells. This suggests that the presence of AgNPs in synergy with metabolites found in the PA plant enhances the biological activity of PA-AgNPs. The observable activities demonstrated by PA-AgNPs are crucial for the development of new therapeutic drugs for cancer diagnostics. Consequently, a more viable approach utilizing plant extracts with a faster and more stable metal ion reduction rate for nanoparticle synthesis is considered to be more favorable. As part of our future plan, it will be fascinating to optimize PA-AgNPs synthesis and research the molecular docking process to develop target-specific treatments.

Supplementary Information The online version contains supplementary material available at https://doi.org/10.1007/s10904-024-03100-9.

Acknowledgements This study was supported by the National Research Foundation (NRF) Postdoctoral Fellowship (Grant number: PSTD2204193734). The authors would like to thank the College of Agriculture and Environmental Sciences (CAES) and the Institute for Nanotechnology and Water Sustainability (iNanoWS) through the University of South Africa (UNISA) for their support.

Author Contributions Project conceptualization, design, experimentation, parameter analysis, and figures and interpretation completed by J.O.O, A.O.O, G.K.M, A.O.A, H.T.M. T.A.M and S.L.L revised the manuscript. All authors reviewed the manuscript.

Funding Open access funding provided by University of South Africa.

Data Availability No datasets were generated or analysed during the current study.

Declarations

Competing Interests The authors declare no competing interests.

References

1. S.A. Petropoulos, A. Karkanis, N. Martins, I.C.F.R. Ferreira, Food Chem. Toxicol. **114**, 155 (2018)
2. M. Sohaib, F.N.I. Al-Barakah, H.M. Migdadi, F.M. Husain, Saudi J. Biol. Sci. **29**, 111 (2022)
3. O.Y. Farouk, J.R. Fahim, E.Z. Attia, M.S. Kamel, South. Afr. J. Bot. **163**, 659 (2023)
4. C.B. Rohal, C. Cranney, E.L.G. Hazelton, K.M. Kettenring, Ecol. Evol. **9**, 13835 (2019)
5. J. Srivastava, S.J.S. Kalra, R. Naraian, Appl. Water Sci. **4**, 193 (2014)
6. M. Machaka, J. Khatib, S. Baydoun, A. Elkordi, J.J. Assaad, Buildings 12, (2022)
7. S. Wichmann, J.F. Köbbing, Ind. Crops Prod. **77**, 1063 (2015)
8. C. William, Sturtevant, *Handbook of North American Indians: Great Basin* (1984)
9. D. Unaipon, *Legendary Tales of the Australian Aborigines* (2001)
10. H. Brix, S. Ye, E.A. Laws, D. Sun, G. Li, X. Ding, H. Yuan, G. Zhao, J. Wang, S. Pei, Ecol. Eng. **73**, 760 (2014)
11. Z.G. Qian, L.F. Jiang, Carbohydr. Polym. **111**, 356 (2014)
12. J. Vymazal, T. Březinová, Chem. Eng. J. **290**, 232 (2016)
13. Y. Lei, L. Carlucci, H. Rijnaarts, A. Langenhoff, Int. J. Phytorem. **25**, 82 (2023)
14. C. Ferrario, C. Peruzzi, A. Cislaghi, S. Polesello, S. Valsecchi, R. Lava, F. Zanon, G. Santovito, A. Barausse, M. Bonato, Water (Switzerland) **14**, (2022)
15. C.A. Odinga, A. Kumar, M.S. Mthembu, F. Bux, F.M. Swalaha, Desalin. Water Treat. **169**, 120 (2019)
16. S.H.K.S.R.L.S. J., S. N. S. H. H. L. Y. K. K. and E.-H. S. Chang Woo Ha. Korean J. Plant. Resour. **33**, 604 (2020)
17. M.J.Y. L., Z. C. C. Z. Y. Z. J. F. Song Chen. Z. Naturforsch. **68**, 439 (2013)
18. Y. Chen, L. Li, L.R. Jiang, J.Y. Tan, L.N. Guo, X.L. Wang, W. Dong, W.B. Wang, J.K. Sun, B. Song, Nat. Prod. Res. **36**, 1454 (2022)
19. M.O. Sim, J.R. Ham, M.K. Lee, Biomed. Pharmacotherapy. **93**, 165 (2017)
20. A.O. Oladipo, J.O. Unuofin, S.L. Lebelo, T.A.M. Msagati, Pharmaceutics. **14**, 2541 (2022)
21. N.A.S. Ismail, J.X. Lee, F. Yusof, Antioxidants. **11**, 1 (2022)
22. S.J. Mahlo, K. Garland, O. More, · Adewale, Oladipo, Sogolo, L. Lebelo, Discover Applied Sciences 6, 62 (123AD)
23. V. Grasmik, M. Breisch, K. Loza, M. Heggen, M. Köller, C. Sengstock, M. Epple, RSC Adv. **8**, 38582 (2018)
24. P. Singh, K.R.B. Singh, J. Singh, S.N. Das, R.P. Singh, RSC Adv. **11**, 18050 (2021)
25. J.O. Adeyemi, A.O. Oriola, D.C. Onwudiwe, A.O. Oyedeji, Biomolecules 12, (2022)
26. M. Hosny, M. Fawzy, O.M. El-Borady, A.E.D. Mahmoud, Adv. Powder Technol. **32**, 2268 (2021)
27. A.O. Oladipo, S.I.I. Iku, M. Ntwasa, T.T.I. Nkambule, B.B. Mamba, T.A.M. Msagati, J. Drug Deliv Sci. Technol. **57**, 101749 (2020)

28. B.B. Kocabas, A. Attar, S.A. Yuka, M.A. Yapaoz, Bioorg. Chem. **133**, (2023)
29. A.O. Oladipo, O.S. Oluwafemi, S.P. Songca, A. Sukhbaatar, S. Mori, J. Okajima, A. Komiya, S. Maruyama, T. Kodama, Sci. Rep. **7**, 45459 (2017)
30. S.K. Nagaraja, R.S. Kumar, B. Chakraborty, H. Hiremath, A.I. Almansour, K. Perumal, P.V. Gunagambhire, S. Nayaka, Appl. Nanosci. (Switzerland). **13**, 3073 (2023)
31. K.N. Shashiraj, A. Hugar, R.S. Kumar, M. Rudrappa, M.P. Bhat, A.I. Almansour, K. Perumal, S. Nayaka, Bioengineering 10, (2023)
32. H.H. Math, K.N. Shashiraj, R.S. Kumar, M. Rudrappa, M.P. Bhat, D.S. Basavarajappa, A.I. Almansour, K. Perumal, S. Nayaka, Inorganics (Basel) **11**, (2023)
33. J.O. Unuofin, G.A. Otunola, A.J. Afolayan, J. Evid. Based Integr. Med. **23**, 1 (2018)
34. M.O. Jimoh, A.J. Afolayan, F.B. Lewu, Sci. Rep. **9**, 1 (2019)
35. J.O. Unuofin, A.O. Oladipo, T.A.M. Msagati, S.L. Lebelo, S. Meddows-Taylor, G.K. More, Arab. J. Chem. **13**, 6639 (2020)
36. J.O. Unuofin, G.A. Otunola, A.J. Afolayan, Processes 7, (2019)
37. G.K. More, C.R. Chokwe, and S. Meddows-Taylor Heliyon **7**, (2021)
38. A.O. Oladipo, J.O. Unuofin, S.I.I. Iku, T.T.I. Nkambule, B.B. Mamba, T.A.M. Msagati, Arab. J. Chem. **14**, 103344 (2021)
39. A. Lewinska, J. Adamczyk-Grochala, E. Kwasniewicz, A. Deregowska, E. Semik, T. Zabek, M. Wnuk, Redox Biol. **14**, 20 (2018)
40. M.D. Cantú, D.R. Toso, C.A. Lacerda, F.M. Lanças, E. Carrilho, M.E.C. Queiroz, Anal. Bioanal Chem. **386**, 256 (2006)
41. I. Rahayu, K.H. Timotius, Molecules **27**, (2022)
42. H.S.A. El-Zahabi, E.S. Nossier, S.M. Mousa, H. Hassan, A.S.G. Shalaby, R.K. Arafa, Arch. Pharm. (Weinheim) **355**, (2022)
43. X.F. Shang, S.L. Morris-Natschke, Y.Q. Liu, X. Guo, X.S. Xu, M. Goto, J.C. Li, G.Z. Yang, K.H. Lee, Med. Res. Rev. **38**, 775 (2018)
44. P. Cui, M. Cai, Y. Meng, Y. Yang, H. Song, Y. Liu, Q. Wang, Sci. Rep. **12**, (2022)
45. Y.F. Jiao, M. Lu, Y.P. Zhao, N. Liu, Y.T. Niu, Y. Niu, R. Zhou, J.Q. Yu, Molecules 23, (2018)
46. A.G. Soman, J.B. Gloer, B. Koster, D. Malloch, J. Nat. Prod. **62**, 659 (1999)
47. B.W.L. Santos, D.C. Moreira, T.K.D.S. Borges, E.D. Caldas, Molecules **27**, (2022)
48. R.G. dos Santos, F.L. Osório, J.A.S. Crippa, J.E.C. Hallak, Revista Brasileira De Psiquiatria. **38**, 65 (2016)
49. M. Wlodarska, C. Luo, R. Kolde, E. d'Hennezel, J.W. Annand, C.E. Heim, P. Krastel, E.K. Schmitt, A.S. Omar, E.A. Creasey, A.L. Garner, S. Mohammadi, D.J. O'Connell, S. Abubucker, T.D. Arthur, E.A. Franzosa, C. Huttenhower, L.O. Murphy, H.J. Haiser, H. Vlamakis, J.A. Porter, R.J. Xavier, Cell. Host Microbe. **22**, 25 (2017)
50. S. Kumar, P. Shah, S.K. Tripathi, S.I. Khan, I.P. Singh, Med. Chem. (Los Angeles). **18**, 949 (2022)
51. S. Tehreem, S. Rahman, M.S. Bhatti, R. Uddin, M.N. Khan, S. Tauseef, H.R. El-Seedi, A. Bin Muhsinah, J. Uddin, S.G. Musharraf, Molecules 26, (2021)
52. A.L. Carreño Otero, L.Y. Vargas Méndez, J.E. Duque L., and, V.V. Kouznetsov, Eur. J. Med. Chem. **78**, 392 (2014)
53. C. Huang, C. Yang, W. Zhang, Y. Zhu, L. Ma, Z. Fang, C. Zhang, J. Antibiot. **72**, 311 (2019)
54. M.O. Sim, J.R. Ham, H.I. Lee, K. Il, Seo, M.K. Lee, Chem. Biol. Interact. **216**, 9 (2014)
55. T. Saito, T. Dai, R. Asano, Oncol. Lett. **5**, 1068 (2013)
56. D. Wang, X. Wang, X. Li, L. Jiang, Z. Chang, Q. Li, Mater. Sci. Eng., C **107**, (2020)
57. M. Wei, Y. Wu, H. Liu, C. Xie, Drug Des. Devel Ther. **14**, 395 (2020)
58. J.H. Kim, K. Kim, W. Kim, Sci. Rep. **10**, (2020)
59. D. Yu, M. Shi, J. Bao, X. Yu, Y. Li, W. Liu, Fitoterapia. **112**, 244 (2016)
60. W. Xiao, S. Li, S. Wang, C.T. Ho, J. Food Drug Anal. **25**, 43 (2017)
61. M. Zhao, K.G. Linghu, L. Xiao, T. Hua, G. Zhao, Q. Chen, S. Xiong, L. Shen, J. Yu, X. Hou, E. Hao, Z. Du, J. Deng, G. Bai, X. Chen, L. Li, P. Li, H. Yu, Food Res. Int. **160**, (2022)
62. K.K. Chiruvella, A. Mohammed, G. Dampuri, R. Gopal Ghanta, S.C. Raghavan, G. Gopal, *Phytochemical and Antimicrobial Studies of Methyl Angolensate and Luteolin-7-O-Glucoside Isolated from Callus Cultures of Soymida Febrifuga* (2007)
63. A. Çakir, A. Mavi, C. Kazaz, A. Yildirim, İrfan Küfrevioğlu. Turk. J. Chem. **30**, 483 (2006)
64. C. Hu, D.D. Kitts, *Luteolin and Luteolin-7-O-Glucoside from Dandelion Flower Suppress INOS and COX-2 in RAW264.7 Cells* (Kluwer Academic, 2004)
65. N. Hasan, H. Osman, S. Mohamad, W.K. Chong, K. Awang, A.S.M. Zahariluddin, Pharmaceuticals. **5**, 882 (2012)
66. F. Peng, L. Xiong, C. Peng, Front. Pharmacol. **11**, (2020)
67. K.M. Marulasiddaswamy, B.R. Nuthan, S. Channarayapatna-Ramesh, S.N. Bajpe, S. Sekhar, K.R. Kini, J. Appl. Pharm. Sci. **11**, 112 (2021)
68. R. Tundis, M. Bonesi, F. Menichini, M.R. Loizzo, F. Conforti, G. Statti, F.M. Pirisi, F. Menichini, Nat. Prod. Commun. **7**, 1015 (2012)
69. H.J. Park, H.S. Shim, A.R. Han, E.K. Seo, K.R. Kim, B.H. Han, I. Shim, Curr. Issues Mol. Biol. **44**, 1407 (2022)
70. S. Shreya, D. Kasote, D. Mohapatra, G.G. Naik, S.K. Guru, N. Sreenivasulu, Y. Sharma, A.N. Sahu, Appl. Biochem. Biotechnol. **195**, 4602 (2023)
71. Y.F. Tan, R.Q. Wang, W.T. Wang, Y. Wu, N. Ma, W.Y. Lu, Y. Zhang, X.P. Zhang, Pharm. Biol. **59**, 884 (2021)
72. E.O. Kim, T.K. Kwon, S.W. Choi, J. Med. Food. **17**, 519 (2014)
73. H. Gaurav, D. Yadav, A. Maurya, H. Yadav, R. Yadav, A.C. Shukla, M. Sharma, V.K. Gupta, J. Palazon, Molecules **28**, (2023)
74. P. Taslimi, İ. Gulçin, J. Food Biochem. **42**, (2018)
75. B. Schlegel, U. Luhmann, A. Hartl, U. Grafe, J. Antibiot. (Tokyo) **53**, (2000)
76. S.M. Moon, S.A. Lee, J.H. Hong, J.S. Kim, D.K. Kim, C.S. Kim, Int. Immunopharmacol. **56**, 179 (2018)
77. Y.T. Oh, J.Y. Lee, J. Lee, J.H. Lee, J.E. Kim, J. Ha, I. Kang, Neurosci. Lett. **474**, 148 (2010)
78. S.E. El-Gengaihi, E.E. Hassan, M.A. Hamed, H.G. Zahran, M.A. Mohammed, J. Diet. Suppl. **10**, 39 (2013)
79. Y. Njankouo Ndam, M.A. Nyegue, P. Mounjouenpou, G. Kansci, M.J. Kenfack, E.E. Eugène, J. Food Process. Preserv **44**, (2020)
80. D. Wigati, K. Anwar, Sudarsono, A.E. Nugroho, J. Evid. Based Complement. Altern. Med. **22**, 107 (2017)
81. T. Napiroon, M. Bacher, H. Balslev, K. Tawaitakham, W. Santimaleeworagun, S. Vajrodaya, J. Appl. Pharm. Sci. **8**, 1 (2018)
82. P. Kashyap, H. Ram, S.D. Shukla, S. Kumar, Neurosci. Insights **15**, (2020)
83. K.M. Sakthivel, S. Vishnupriya, L.C.P. Dharshini, R.R. Rasmi, B. Ramesh, J. Pharm. Pharmacol. **74**, 147 (2022)
84. J.H. Jang, J.E. Park, J.S. Han, Nutr. Res. **74**, 52 (2020)
85. X. Ao, J. Yan, S. Liu, S. Chen, L. Zou, Y. Yang, L. He, S. Li, A. Liu, K. Zhao, Food Chem. **374**, (2022)
86. C. juan Fang, X. juan Rong, W. Jiang, X. Chen, and Y. ling Liu, Heliyon 9, (2023)
87. M. Shan, S. Yu, H. Yan, S. Guo, W. Xiao, Z. Wang, L. Zhang, A. Ding, Q. Wu, S.F.Y. Li, Molecules 22, (2017)
88. W. Liu, G. Li, C. Hölscher, L. Li, Rev. Neurosci. **26**, 371 (2015)

89. C.H. Peng, C.N. Huang, C.J. Wang, *The Anti-Tumor Effect and Mechanisms of Action of Penta-Acetyl Geniposide* (2005)
90. F.L. Ge, L.L. Si, Y. Yang, Y.H. Li, Z.L. Lv, W.H. Liu, H. Liao, J. Wang, J. Zou, L. Li, H. Li, Z.L. Zhang, J.B. Wang, X.C. Lu, D.P. Xu, Z.F. Bai, Y. Liu, X.H. Xiao, Front. Pharmacol. **12**, (2021)
91. D.S. Duarte, M.F. Dolabela, C.E. Salas, D.S. Raslan, A.B. Oliveiras, A. Nenninger, B. Wiedemann, H. Wagner, J. Lombardi, M.T.P. Lopes, J. Pharm. Pharmacol. **52**, 347 (2010)
92. S. Caporali, A. De Stefano, C. Calabrese, A. Giovannelli, M. Pieri, I. Savini, M. Tesauro, S. Bernardini, M. Minieri, A. Terrinoni, Nutrients 14, (2022)
93. X. Li, W. Zhu, L. Yang, D. Fei, J. Fan, L. Du, Y. Liu, Nat. Prod. Res. **27**, 1657 (2013)
94. A.K. Giri, B. Jena, B. Biswal, A.K. Pradhan, M. Arakha, S. Acharya, L. Acharya, Sci. Rep. **12**, (2022)
95. O.M. El-Borady, M. Fawzy, M. Hosny, Appl. Nanosci. (Switzerland). **13**, 3149 (2023)
96. S. Donga, S. Chanda, Artif. Cells Nanomed. Biotechnol. **49**, 292 (2021)
97. A. Ganesh Kumar, E. Pugazhenthi, P. Sankarganesh, C. Muthusamy, M. Rajasekaran, E. Lokesh, A. Khusro, G. Kavya, Biomass Convers Biorefin (2023)
98. N. Konappa, A.C. Udayashankar, N. Dhamodaran, S. Krishnamurthy, S. Jagannath, F. Uzma, C.K. Pradeep, S. De Britto, S. Chowdappa, S. Jogaiah, Biomolecules 11, (2021)
99. A.H. Labulo, O.A. David, A.D. Terna, Chem. Pap. **76**, 7313 (2022)
100. J. Flieger, W. Franus, R. Panek, M. Szymańska-Chargot, W. Flieger, M. Flieger, P. Kołodziej, Molecules 26, (2021)
101. A. Demirbas, B.A. Welt, I. Ocsoy, Mater. Lett. **179**, 20 (2016)
102. F.Ö. Küp, S. Çoşkunçay, F. Duman, Mater. Sci. Eng., C **107**, (2020)
103. G.A. Otunola, A.J. Afolayan, E.O. Ajayi, S.W. Odeyemi, Pharmacogn Mag. **13**, S201 (2017)
104. G. Das, J.K. Patra, N. Basavegowda, C.N. Vishnuprasad, H.S. Shin, Int. J. Nanomed. **14**, 4741 (2019)
105. J. He, C. Gong, J. Qin, M. Li, S. Huang, Nanoscale Res. Lett. **14**, (2019)
106. P. Paramasivan, J.D. Kumar, R. Baskaran, C.F. Weng, V.V. Padma, Cancer Drug Resist. **3**, 647 (2020)
107. A.O. Oladipo, J.O. Unuofin, S.I.I. Iku, T.T.I. Nkambule, B.B. Mamba, T.A.M. Msagati, Int. J. Pharm. **602**, 120661 (2021)
108. E.O. Mikhailova, J. Funct. Biomater. **11**, (2020)
109. A.A. Al-kawmani, K.M. Alanazi, M.A. Farah, M.A. Ali, W.A.Q. Hailan, F.M.A. Al-Hemaid, J. King Saud Univ. Sci. **32**, 2480 (2020)
110. K. Marković, A. Kesić, M. Novaković, M. Grujović, D. Simijonović, E.H. Avdović, S. Matić, M. Paunović, M. Milutinović, D. Nikodijević, O. Stefanović, Z. Marković, RSC Adv. **14**, 4591 (2024)
111. A.B. Thakkar, R.B. Subramanian, V.R. Thakkar, S.V. Bhatt, S. Chaki, Y.H. Vaidya, V. Patel, P. Thakor, Heliyon 10, (2024)